IVYSPRING INTERNATIONAL PUBLISHER

Theranostics

2017; 7(15): 3715-3731. doi: 10.7150/thno.19678

Research Paper

# Selective Targeting of a Novel Vasodilator to the Uterine Vasculature to Treat Impaired Uteroplacental Perfusion in Pregnancy

Natalie Cureton[1, 2], Iana Korotkova[1, 2], Bernadette Baker[1, 2], Susan Greenwood[1, 2], Mark Wareing[1, 2], Venkata R Kotamraju[3], Tambet Teesalu[3, 4], Francesco Cellesi[5, 6], Nicola Tirelli[7], Erkki Ruoslahti[3], John D Aplin[1, 2], Lynda K Harris[1, 2, 7]✉

1. Maternal and Fetal Health Research Centre, Division of Developmental Biology and Medicine, University of Manchester, Manchester, UK;
2. Academic Health Science Centre, St Mary's Hospital, Oxford Road, Manchester, M13 9WL, UK;
3. Cancer Center, Sanford–Burnham Medical Research Institute, 10901 N. Torrey Pines Road, La Jolla, CA 92037, USA and Center for Nanomedicine and Department of Cell, Molecular and Developmental Biology, University of California, Santa Barbara, Santa Barbara, CA 93106–9610, USA;
4. Laboratory of Cancer Biology, Institute of Biomedicine, Centre of Excellence for Translational Medicine, University of Tartu, Tartu, Estonia;
5. Dipartimento di Chimica, Materiali ed Ingegneria Chimica "G. Natta". Politecnico di Milano, Via Mancinelli 7, 20131 Milan, Italy;
6. Fondazione CEN – European Centre for Nanomedicine, Piazza Leonardo da Vinci 32, 20133 Milan, Italy;
7. Division of Pharmacy and Optometry, University of Manchester, Stopford Building, Oxford Road, Manchester, M13 9PT, UK.

✉ Corresponding author: Dr Lynda Harris (lynda.k.harris@manchester.ac.uk); Division of Pharmacy and Optometry, University of Manchester, Stopford Building, Oxford Road, Manchester, M13 9PT, UK.



Received: 2017.02.15; Accepted: 2017.06.12; Published: 2017.08.29

## Abstract

Fetal growth restriction (FGR) in pregnancy is commonly caused by impaired uteroplacental blood flow. Vasodilators enhance uteroplacental perfusion and fetal growth in humans and animal models; however, detrimental maternal and fetal side effects have been reported. We hypothesised that targeted uteroplacental delivery of a vasodilator would enhance drug efficacy and reduce the risks associated with drug administration in pregnancy. Phage screening identified novel peptides that selectively accumulated in the uteroplacental vasculature of pregnant mice. Following intravenous injection, the synthetic peptide CNKGLRNK selectively bound to the endothelium of the uterine spiral arteries and placental labyrinth *in vivo*; CNKGLRNK-decorated liposomes also selectively bound to these regions. The nitric oxide donor 2-[[4-[(nitrooxy)methyl]benzoyl]thio]-benzoic acid methyl ester (SE175) induced significant relaxation of mouse uterine arteries and human placental arteries *in vitro*; thus, SE175 was encapsulated into these targeted liposomes and administered to healthy pregnant C57BL/6J mice or endothelial nitric oxide synthase knockout ($eNOS^{-/-}$) mice, which exhibit impaired uteroplacental blood flow and FGR. Liposomes containing SE175 (0.44mg/kg) or PBS were administered on embryonic (E) days 11.5, 13.5, 15.5 and 17.5; fetal and placental weights were recorded at term and compared to mice injected with free PBS or SE175. Targeted uteroplacental delivery of SE175 had no effect on fetal weight in C57BL/6J mice, but significantly increased fetal weight and mean spiral artery diameter, and decreased placental weight, indicative of improved placental efficiency, in $eNOS^{-/-}$ mice; free SE175 had no effect on fetal weight or spiral artery diameter. Targeted, but not free SE175 also significantly reduced placental expression of 4-hydroxynonenal, cyclooxygenase-1 and cyclooxygenase-2, indicating a reduction in placental oxidative stress. These data suggest that exploiting vascular targeting peptides to selectively deliver SE175 to the uteroplacental vasculature may represent a novel treatment for FGR resulting from impaired uteroplacental perfusion.

Key words: pregnancy, placenta, nitric oxide, endothelium, vascular biology, drug targeting.

## Introduction

More than five percent of pregnancies are complicated by fetal growth restriction (FGR), where the developing fetus does not reach its full growth potential, resulting in significant maternal and fetal morbidity and/or mortality [1,2]. There is also evidence that being born small or premature can program obesity and increase the risk of adulthood diseases such as cardiovascular disease and type 2 diabetes [3]. Current management strategies are limited to fetal monitoring, and induction of labour when suboptimal growth threatens fetal survival [4]. However, pre-term delivery can exacerbate some of the adverse effects associated with growth restriction [5]. Despite these short and long-term health implications, development of therapeutics for use in pregnancy is hindered by the risk of systemic side effects and lack of interest from the pharmaceutical industry [6,7].

Peptide-mediated targeting of payloads to individual vascular beds has enabled selective delivery of therapeutics to specific organs and tissues [8,9], offering enhanced efficacy and importantly, reducing off-target, systemic side effects [10]. Much of the current research in this area has focussed on delivery of chemotherapeutics to tumours, which has been achieved by targeting specific receptors on the tumour vasculature [11, 12]. A peptide that homes to atherosclerotic plaques has also been identified, which triggers apoptosis of plaque macrophages and reduces plaque hypoxia [13,14]. The villous placenta and surrounding uterine vasculature express a number of cell-surface epitopes common to those observed in the vasculature in solid tumours [15]. Indeed, the placenta has been likened to a solid tumour, exhibiting high rates of proliferation in the first trimester, giving rise to a subset of invasive cells and modulating the maternal immune response. These observations, along with our finding that some peptides which home to tumours can also be exploited for placental targeting [16], led us to seek novel sequences that home to the uteroplacental vasculature.

Abnormal vascular anatomy [17] and impaired myometrial and chorionic plate vascular tone regulation are present in some cases of FGR in humans [18-22]. Reduced uterine and umbilical blood flow alters the diffusion gradient for transfer of small lipophilic solutes such as $O_2$ and $CO_2$ across the placenta [23], thus restricting fetal growth. Moreover, impaired uteroplacental blood flow contributes to FGR in both human and mouse pregnancies [24,25], suggesting that enhancement of flow may provide a means to improve fetal growth *in utero*. Indeed, administration of the vasodilator sildenafil citrate (Viagra™) to pregnant women presenting with FGR improved uteroplacental perfusion, as identified by Doppler ultrasound [26]. Sildenafil citrate also significantly increased fetal weight in the two mouse models of FGR [27-29]; however, maternal administration of sildenafil citrate caused impaired vasorelaxation of fetal abdominal aortas, led to female offspring exhibiting impaired glucose tolerance, and caused the offspring to have elevated blood pressure as adults [27,30,31]. These studies demonstrate the potential side effects of systemic maternal delivery of therapeutics in pregnancy and lend support to the use of targeted drug delivery.

In this study, we have used phage screening to identify novel peptide sequences that selectively bind to the uteroplacental vasculature and created liposomes bearing one such sequence for targeted drug delivery. We have also assessed the ability of a novel vasodilator, 2-[[4-[(nitrooxy)methyl]benzoyl]-thio]-benzoic acid methyl ester (SE175), to relax uterine arteries from pregnant mice and enhance fetal growth *in vivo*. SE175, a nitroxyacylated thiosalicylate, contains a nitric oxide (NO)-donating nitrate group attached to a NO-liberating thiosalicylate [55]; this class of compound was created in an effort to achieve spontaneous release of NO from nitrate groups, based on the evidence that a free thiol (SH) is able to liberate NO from nitrate groups [72]. Esterase breakdown of SE175 allows the thiosalicylate group to self-liberate NO from the nitrate group, thus SE175 should not cause the tolerance that has been observed following repeated administration of traditional nitrates.

We evaluated the effects of SE175 in pregnant wild-type C57BL/6J mice and in endothelial nitric oxide synthase ($eNOS^{-/-}$) knockout mice, which exhibit pre-pregnancy hypertension and a compromised adaptive cardiovascular response to pregnancy: uterine artery remodeling is impaired [32,33] and uteroplacental perfusion is reduced [34]. Offspring are on average 10% lighter than in C57BL/6J mice indicating FGR [35]. No gross structural abnormalities have been reported in $eNOS^{-/-}$ mice but placental nutrient transport is reduced, and placentas exhibit evidence of oxidative stress and uteroplacental hypoxia [36]. Oxidative stress in the mouse placenta leads to the induction of both cyclooxygenase-1 (COX-1) and cyclooxygenase-2 (COX-2), leading to prostaglandin synthesis and elevated rates of apoptosis [37]. Here we demonstrate that targeted delivery of SE175 to the uteroplacental vasculature of $eNOS^{-/-}$ mice enhances fetal growth and reduces placental oxidative stress.

## Methods

### Animal procedures

BALB/c mice (Charles River, USA), C57BL/6J mice (UK) and eNOS mice (UK) were housed and all procedures were performed according to procedures approved by the Animal Research Committees at University of California, Santa Barbara, or in accordance with the UK Animals (Scientific Procedures) Act 1986 at The University of Manchester. Animals had free access to food and water and were maintained on a 12:12 h light–dark cycle at 21–23°C. After mating, the presence of a copulation plug was denoted as embryonic *day 0.5 (E0.5)* of pregnancy.

### Phage display

The T7-select phage display system (EMD Biosciences, USA) was used to construct peptide libraries. Individual phages were cloned according the manufacturer's instructions, as previously described [38,39]. Amplified phages were purified from bacterial lysate by precipitation with PEG-8000 (Sigma Aldrich, MO, USA), caesium chloride gradient ultracentrifugation and dialysis. The identity of the displayed peptides was determined by sequencing the DNA encoding the insert-containing region at the C terminus of the T7 major coat protein gp10 (Eton Bioscience, CA, USA).

### Phage screening

Mouse placentas (E13.5 - E14.5) were harvested, washed in PBS and mechanically dissociated using a Medimachine system (BD Biosciences). The resulting tissue aggregates were incubated with the T7 phage library ($10^{10}$ pfu/mg tissue) in 10 ml DMEM culture medium containing 1% (w/v) BSA (Life Technologies, NY, USA) for 1 h at 4°C on a rotating wheel, then pelleted by centrifugation (400*g*; 5 min). Tissue was washed by centrifugation (400 *g*; 5 X 5 min) in fresh culture medium and lysed in LB bacterial growth medium containing 1% Nonidet P-40 (Sigma Aldrich, MO, USA). Bound phage was quantified by titration and amplified as previously described [38,39]. The *ex vivo* selection process was repeated three times, then the resulting phage pool was injected into the tail vein of a pregnant mouse and allowed to circulate for 30 min. To remove unbound phage, mice were subjected to terminal cardiac perfusion with 30 ml of PBS. The uterus and placentas were harvested and homogenized in LB bacterial growth medium containing 1% (v/v) Nonidet P-40, and bound phage were titered, amplified and purified. Four rounds of *in vivo* screening were performed in total, using pregnant mice between E13.5 and E15.5. Ninety-six individual phage clones from each of the second, third and fourth rounds of screening were subjected to DNA sequencing to determine the identity of their surface peptides.

### Peptide synthesis

Peptides were synthesized at The University of California, Santa Barbara using Fmoc chemistry in a solid–phase synthesizer, were purified by HPLC, and sequences and structures confirmed by mass spectrometry as previously described [38]. Alternatively, they were purchased from Insight Biotechnology, UK.

### Peptide targeting

Individual synthetic peptides (200 µg) labeled with 5(6)–carboxyfluorescein (FAM) were injected into the tail vein of pregnant mice (E11.5–E17.5) and allowed to circulate for 3 h. Following terminal cardiac perfusion with PBS to remove unbound peptide, maternal and fetal tissues were collected for analysis. Organs were snap frozen, or fixed in paraformaldehyde (4% (w/v) in PBS; overnight) and cryoprotected in sucrose solution (30% (w/v) in PBS; 24 h), embedded in OCT (Sakura) and stored at –80 °C. Tissue sections (8 µm) were fixed in ice–cold methanol (15 min), washed in PBS (2 X 5 min), mounted in Vectashield medium containing DAPI (4',6–diamidino–2–phenylindole; Vector Laboratories, Burlingame, USA) and examined on an Olympus Fluoview 500 confocal microscope (Olympus America) or a Zeiss AxioObserver fluorescence microscope (Zeiss, UK). Images were captured at the same exposure so that comparisons of fluorescence intensity could be made between samples.

### Liposome synthesis

Targeted liposomes were prepared by dissolving 1,2-distearoyl-*sn*-glycero-3-phosphocholine (DSPC; 65 µmol/L), cholesterol (30 µmol/L), 1,2-distearoyl-*sn*-glycero-3-phosphoethanolamine-N-[amino(polyethylene glycol)] (DSPE-PEG; 4.5 µmol/L) and DSPE-PEG-maleimide (0.5 µmol/L; Avanti Polar Lipids) in methanol:chloroform (9:1 ratio). Solvent was removed by rotary evaporation to produce a thin lipid film, which was rehydrated with distilled water (2 mL). The resulting suspension was heated to 62°C for 3 h to produce large multilamellar vesicles and extruded eleven times using a 1 mL Mini-Extruder (Avanti Polar Lipids) through a 0.1 µm, 19 mm polycarbonate membrane, surrounded by two 10 mm filter supports in order to produce a unilamellar liposome suspension. Fluorescent targeting peptides (0.27 µmol/L) bearing a cysteine residue on the N-terminus were added to 1 mL of extruded liposome

suspension and allowed to covalently couple with maleimide groups overnight at room temperature via a Michael type addition reaction. Unreacted peptide was removed by dialysis against PBS (8 X 1 litres; 24 h; Slide-A-Lyzer Dialysis Cassettes, MWCO 3.5 kDa) and the suspension stored at 4°C until use. The size (hydrodynamic diameter) distribution (SD) and polydispersity index (PDI) were measured by dynamic light scattering (DLS), and the zeta potential (ZP) was measured by laser Doppler micro-electrophoresis (LDE) (25°C; scattering angle of 173° (Zetasizer Nano ZS, Model ZEN3600, fitted with a 632 nm laser, Malvern Instruments Ltd., UK).

To encapsulate SE175, the lipid film was rehydrated with SE175 (2 mL, 320 µmol/L stock) and the resultant suspension was heated at 62°C for 3 h and extruded, as described above. Fluorescent targeting peptides (0.27 µmol/L) were conjugated to maleimide groups on the liposomal surface via a Michael–type addition reaction. Unreacted peptide was removed by dialysis against PBS and the suspension was stored at 4°C.

Non-targeted liposomes were prepared by dissolving DPSC (65 µmol/L), cholesterol (30 µmol/L), DSPE-PEG (5 µmol/L) in methanol:chloroform (9:1 ratio), followed by the addition of 2.7 µmol/L of fluorescently labelled lipid NBD-DSPE (5 0µL, 0.1 mg/mL stock). As described above, the solvent was removed by rotary evaporation, the lipid film was rehydrated with PBS (2 mL) and the resultant suspension was heated at 62°C for 3 h. The suspension was then extruded using a 1 mL Mini-Extruder through a 0.1 µm, 19 mm polycarbonate membrane, free drug was removed by dialysis against PBS and the suspension was stored at 4°C.

## Validation of liposome targeting *in vivo*

Liposomes (100 µL) decorated with rhodamine-labelled CNKGLRNK peptides and NBD-labelled fluorescent lipids were injected into the tail vein of pregnant mice (E13.5–E15.5) and allowed to circulate for up to 48h. Following terminal cardiac perfusion with PBS to remove unbound liposomes, maternal and fetal tissues were collected for analysis. Organs were fixed in neutral buffered formalin (4% (v/v); overnight), embedded in OCT (RA Lamb, UK) and stored at –80 °C. Tissues sections (8 µm) were fixed in PFA (15 min), washed in PBS (2 X 5 min), mounted in Vectashield mounting medium containing DAPI and examined using a Zeiss AxioObserver fluorescence microscope (Zeiss, UK). Images were captured at the same exposure so that comparisons of fluorescence intensity could be made between samples.

## Human tissue

First trimester placentas were collected following surgical or medical termination of pregnancy. Term placentas (37–42 weeks gestation) were obtained from normal pregnancies within 30 min of vaginal or Caesarean delivery. The study was performed in accordance with North West Local Research Ethical Committee approvals (08/H1010/28; 08/H1010/55) and written informed consent was obtained from all patients. Villous tissue was randomly sampled, washed in serum–free culture medium and dissected into 3 $mm^3$ explants under sterile conditions. Explants were cultured a 1:1 ratio of DMEM and Ham's F12 media (Lonza Biosciences, UK) containing glutamine (2 mmol/L), penicillin (100 IU $ml^{-1}$), streptomycin (100 µg $ml^{-1}$) and 10% (v/v) fetal bovine serum (Life Technologies), in 24 well culture plates pre–coated with agarose (1% (w/v); Sigma Aldrich). Explants were maintained in 20% $O_2$, 5% $CO_2$ at 37 °C for up to 7 days.

## Peptide binding to human placental explants

Rhodamine–labelled peptides (20 µmol/L) were incubated with human first trimester or term placental explants at 37°C for up to 3 h in culture media. Tissue was washed in PBS, fixed in neutral buffered formalin overnight (4% (v/v); pH 7.4), frozen and cryosectioned. Tissues sections (8 µm) were fixed in PFA (15 min), washed in PBS (2 X 5 min), mounted in Vectashield mounting medium containing DAPI and assessed using a Zeiss AxioObserver fluorescence microscope.

## Liposome binding to human placental explants

Peptide-decorated liposomes (100 µL) were cultured with term placental explants (37°C, 95% air, 5% carbon dioxide) for up to 48 h. Tissue was washed in PBS, fixed in neutral buffered formalin overnight (4% (v/v); pH 7.4), frozen and cryosectioned. Tissue sections (8 µm) were fixed in PFA (15 min) and washed in PBS (2 X 5 min). Sections were mounted in Vectashield containing DAPI and visualised using a Zeiss AxioObserver fluorescence microscope.

## Wire myography

Pregnant female mice were euthanized by cervical dislocation at E18.5. A surgical laparotomy was performed on the dam to expose the uterine horn. The horn was pinned out as previously described [36] and main loop uterine artery carefully excised using a dissection microscope (model S6E, Leica, UK). The dissected artery was trimmed into approximately 40 µm length sections and kept in cold physiological salt solution prior to mounting on the wire myograph. Dissected arterial sections were mounted by inserting

two 40 μm steel wires into the lumen, which were secured in the jaws of a Multi Myograph System 610M (Danish Myo Technology A/S, Denmark) as previously described [40]. Arterial section diameter was measured using a calibrated eyepiece graticule and equilibrated to physiological conditions in 6 mL PSS, warmed to 37°C and gassed with 20% $O_2$ / 5% $CO_2$ / balanced with $N_2$ (BOC Gases, Worsley, UK). Vessels were normalised to ensure that arterial sections of different diameters had the same resting tension, as previously described [41], and were left to equilibrate for 20 minutes.

Chorionic plate biopsies taken from human term placentas were placed into ice-cold PSS. Small chorionic plate arterial branches originating from the main umbilical arteries were identified, dissected and trimmed into approximately 40 μm length sections. Vessels were mounted on a wire myograph and normalised as described above.

Human chorionic plate and mouse uterine arteries were exposed to a high potassium salt solution for 5 min to determine maximal smooth muscle contraction, before being washed twice with PSS. Arterial sections were left to re-equilibrate for 20 min, before being exposed to phenylephrine (PE, $10^{-5}$ mol/L) for 10 min to determine maximal contraction. After 10 min, arterial sections were exposed to acetylcholine (ACh, $10^{-5}$ mol/L) to determine maximal relaxation, before being washed twice with PSS and left to equilibrate for 20 min. PE exposure was then repeated and relaxation to SE175 determined, following the application of incremental doses ($10^{-9}$ – $10^{-5}$ M, 2 min intervals). Equivalent concentrations of DMSO (vehicle control) and no treatment (time control) were assessed in parallel. When targeted liposomes containing SE175-were applied to arterial sections, the extent of relaxation to a single dose (100 μl) of SE175 was determined. Relaxation data were expressed as percentage relaxation of maximum pre-constriction to PE. Myodata software (version 2.02; Myonic Software, National Instruments Corporation, USA) was used to visualise and interpret data.

## Measurement of system A activity

After 6 days in culture, term placental explants were treated with SE175 (10 μM), SNAP (10 μM) or DMSO (0.6 %; vehicle control) and system A activity was measured on day 7. Explants were incubated for 30, 60 or 90 min in either $Na^+$-containing or $Na^+$-free Tyrode's buffer (NaCl replaced by an equimolar concentration of choline chloride) containing 0.5 μCi/ml $^{14}$C-MeAIB (~8.5 μM) at 37 °C. The explants were then washed in ice-cold Tyrode's buffer and lysed in $dH_2O$ for 16–18 h at room temperature (RT). The radioactive content of the water lysate was measured using a β-counter. $Na^+$-dependent system A activity was calculated by subtracting uptake in $Na^+$-free Tyrode's from that in $Na^+$-containing Tyrode's, with correction for fragment protein content, measured using Bio-Rad protein assay (Bio-Rad Laboratories Ltd, Hertfordshire, UK).

## Liposome treatment study

Time-mated, pregnant C57 and eNOS$^{-/-}$ mice were intravenously injected with 100 μL of either PBS, CNKGLRNK-decorated liposomes containing PBS, free SE175 (320 μmol/L, approximately 0.44 mg/kg) or CNKGLRNK-decorated liposomes containing SE175 (320 μmol/L; approximately 0.44 mg/kg) on E11.5, E13.5, E15.5 and E17.5. Mice were sacrificed by cervical dislocation at E18.5 and the following measurements taken: litter size, number of resorptions, fetal weight, placental weight, maternal kidney weight, maternal spleen weight and maternal heart weight. Organs were fixed in neutral buffered formalin (4% (v/v), pH 7.4; overnight) for paraffin embedding. The weight and behaviour of treated dams were continuously monitored to detect signs of toxicity or distress. Gross morphological analysis of fetuses and maternal organs was undertaken to detect physical deformities or abnormalities associated with treatment.

## Immunostaining

Tissue sections (5 μm) were deparaffinised in Histoclear and alcohol and then rehydrated in $dH_2O$. Slides were microwaved in antigen retrieval buffer (sodium citrate buffer (0.01 mol/L), containing 0.05% (v/v) Tween 20 (pH 6.0), 20 min), followed by cooling for 10 min. After cooling, tissue sections were incubated with hydrogen peroxidase (3% (w/v), 10 min) to block endogenous peroxide activity, washed 3 times in Tris-buffered saline (TBS) and incubated with bovine serum albumin (BSA; 5% (w/v) in TBS, 30 min) to block non-specific binding. Tissue sections were then incubated with primary antibodies (Table 1) or control IgG (matched concentration; Sigma Aldrich) overnight at 4°C. Tissue sections were washed 3 times (TBS; 5 min) and incubated at room temperature with a swine anti-rabbit or goat anti-mouse secondary antibody (1:200; DakoCytomation A/S) for 30 min. Tissue sections were then washed 3 times (TBS; 5 min) and incubated at room temperature with avidin peroxidase (5 μg/mL in TBS, 30 min; Sigma Aldrich). Tissue sections were then washed with $dH_2O$, incubated for 2-10 min with diaminobenzidine (DAB; 0.05% (w/v); Sigma Aldrich) and urea hydrogen peroxide (0.015% (v/v); Sigma Aldrich, UK) and washed again with

$dH_2O$. Tissue sections were then counterstained with filtered Harris's hematoxylin, dehydrated in alcohol and Histoclear and mounted in DPX mountant (Sigma Aldrich, UK). All sections were stained in the same run to allow direct comparison between groups.

**Table 1.** Primary antibodies

| Antigen | Host Species | Target Species | Supplier | Dilution |
|---|---|---|---|---|
| COX-1 aa 274 – 288 #160109 | Rabbit | Mouse | Cayman Chemicals, UK | 1:250 |
| COX-2 aa 584 – 598 #160126 | Rabbit | Mouse | Cayman Chemicals, UK | 1:1000 |
| HNE #HNE11-S | Rabbit | Mouse | Alpha Diagnostics, UK | 1:500 |
| Ki67 (clone MIB-1) | Mouse | Human | DakoCytomation A/S, Denmark | 1:250 |
| M30 CytoDEATH | Mouse | Human | Roche Diagnostics GmbH, UK | 1:100 |
| IgG #I8140 | Rabbit | Mouse | Sigma Aldrich, UK | Matched |
| IgG #I8765 | Mouse | Human | Sigma Aldrich, UK | Matched |

For quantitative analysis of immunostaining, a minimum of three treated mice per group were selected at random and three placentas per mouse were immunostained in the same run for direct comparison of images. Nine images were taken per placenta using the same exposure settings, on the Olympus B641 Light Microscope using Image-Pro Plus 7 software, equating to twenty-seven images per mouse (taken as n = 1). Images were then analysed using TissueGnostics HistoQuest® Analysis Software. Hematoxylin (nuclear stain) total area and DAB (antibody stain) total area were determined and a ratio of DAB area to hematoxylin area calculated to control for tissue area. The mean luminal diameter of individual spiral arteries was also quantified using HistoQuest® software. For human tissue, six random images were taken of each explant using the same exposure settings and analysed using the HistoQuest software. The percent of proliferating and apoptotic cells was calculated by dividing the total area of DAB-positive nuclei (Ki67 or M30 positive cells) by the total area of haematoxylin-positive nuclei and multiplying by 100.

### Statistical analysis

All data were analysed using GraphPad Prism software (Version 7). Myography data were analysed using two-way analysis of variance with Bonferroni *post hoc* test for comparisons between groups. System A activity was analysed using linear regression to assess differences in the rate of $Na^+$-dependent $^{14}C$-MeAIB uptake between treatments. Unless otherwise stated, all other data were analysed using one-way ANOVA or a Kruskal Wallis test with Dunnett *post hoc* test for comparisons between groups. Frequency distribution curves were generated by performing non-linear regression on fetal / placental weight histograms. Unless otherwise stated, data are shown as mean ± SEM and significance was taken as $P < 0.05$.

## Results

### The placental-homing peptide NKGLRNK selectively binds to the uteroplacental vasculature

To isolate placental homing phages, mouse placental tissue (E13.5-14.5) was incubated with a T7 bacteriophage library containing about $10^8$ individual clones, in which each clone displays multiple copies of a unique, random 7-mer peptide on its surface. Each sequence is represented ~100 times, thus the starting library contained approximately $10^{10}$ phage. During the three rounds of *ex vivo* phage selection, the phage library collapsed by three orders of magnitude ($10^7$ to $10^4$; Figure 1A), as previously reported [39]; however, subsequent rounds of *in vivo* screening led to phage enrichment (Figure 1B). Ninety-six phage clones from the second, third and fourth rounds of *in vivo* screening were sequenced and the surface peptide NKGLRNK (NKG) was the most highly represented. To confirm that this sequence selectively targets the mouse placenta *in vivo*, synthetic peptide labelled with 5(6)–carboxyfluorescein (FAM) was injected intravenously into pregnant mice. FAM-NKG bound to the intima of decidual spiral arteries (SA) and the vasculature of the placental labyrinth (Lab), but not to the junctional zone (JZ) between E10.5 and E17.5 (Figure 1C-E). Analysis of maternal tissues confirmed that FAM-NKG did not accumulate in the vascular bed of any other major organ, although small, discrete areas of fluorescence were sometimes observed in the kidney and spleen (Figure 1F-K).

### Homing peptide-decorated liposomes preferentially home to the uteroplacental vasculature

To conjugate the homing peptide to the surface of liposomes it was necessary to add a cysteine residue to the N-terminus: CNKGLRNK (CNKG). To ensure that tissue binding was not affected, excised mouse uterine arteries were incubated with rhodamine (Rh)-labelled peptide (20 µmol/L) for up to 3 h. Rh-CNKG bound to, and accumulated within, the vascular endothelium and underlying smooth muscle layers (Figure 2A, B), as observed *in vivo*. Rh-CNKG-coupled liposomes containing PBS or SE175 were synthesised and characterised; PBS-loaded liposomes had a mean diameter of 159.8 ±

1 nm, a mean zeta potential of -0.6 ± 0.4 mV and a polydispersity index of 0.065. SE175-loaded liposomes had a diameter of 164.2 ± 1 nm, a zeta potential of -1.0 ± 0.6 mV and a polydispersity index of 0.049 (Figure 2C, D). The liposomes demonstrated excellent stability over 28 days, with mean particle size and polydispersity index remaining constant during this time.

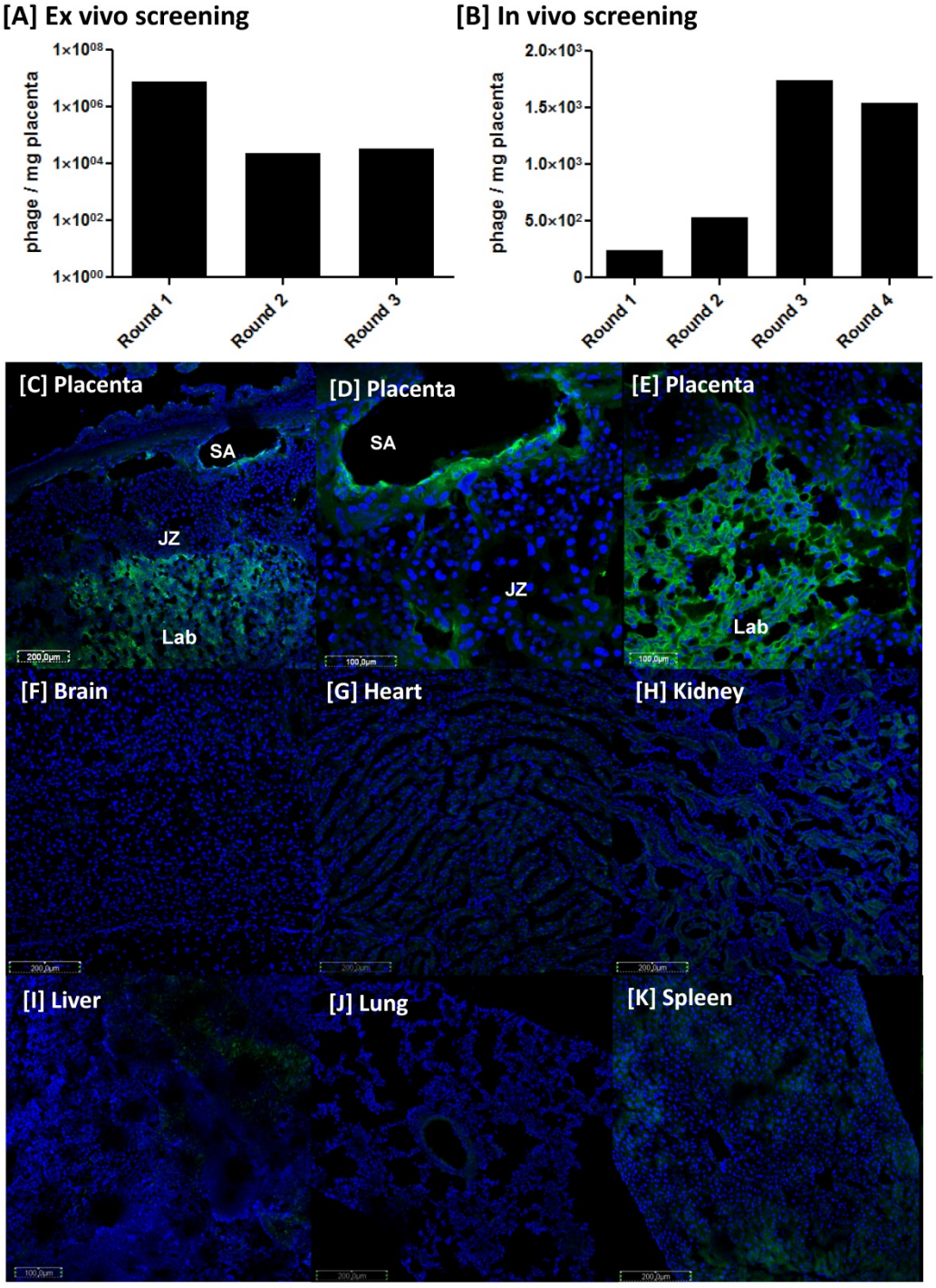


**Figure 1**. **Identification of the placental-homing peptide NKGLRNK [A]** Mouse placental tissue was incubated with a T7 bacteriophage library and bound phages were titered, amplified and purified. Phage titer (pfu/mg tissue) was measured using a plaque-forming assay (n=3). **[B]** Following 3 rounds of *ex vivo* selection, the resulting phage pool was injected into the tail vein of a pregnant mouse. Placentas were harvested and bound phage pools were titered, amplified and purified. Four rounds of *in vivo* screening were performed in total; phage titer is expressed as pfu/mg tissue (n = 3). **[C-E]** NKGLRNK labelled with 5(6)-carboxyfluorescein (FAM; 200 µg) was injected into the tail vein of pregnant mice (n = 5; E10.5 - E17.5). Following cardiac perfusion to remove unbound peptide, placentas were harvested and assessed by fluorescence microscopy. Representative images are shown. FAM-labelled peptides, green; DAPI (nuclei), blue. JZ = junctional zone; Lab = labyrinth; SA = spiral artery.

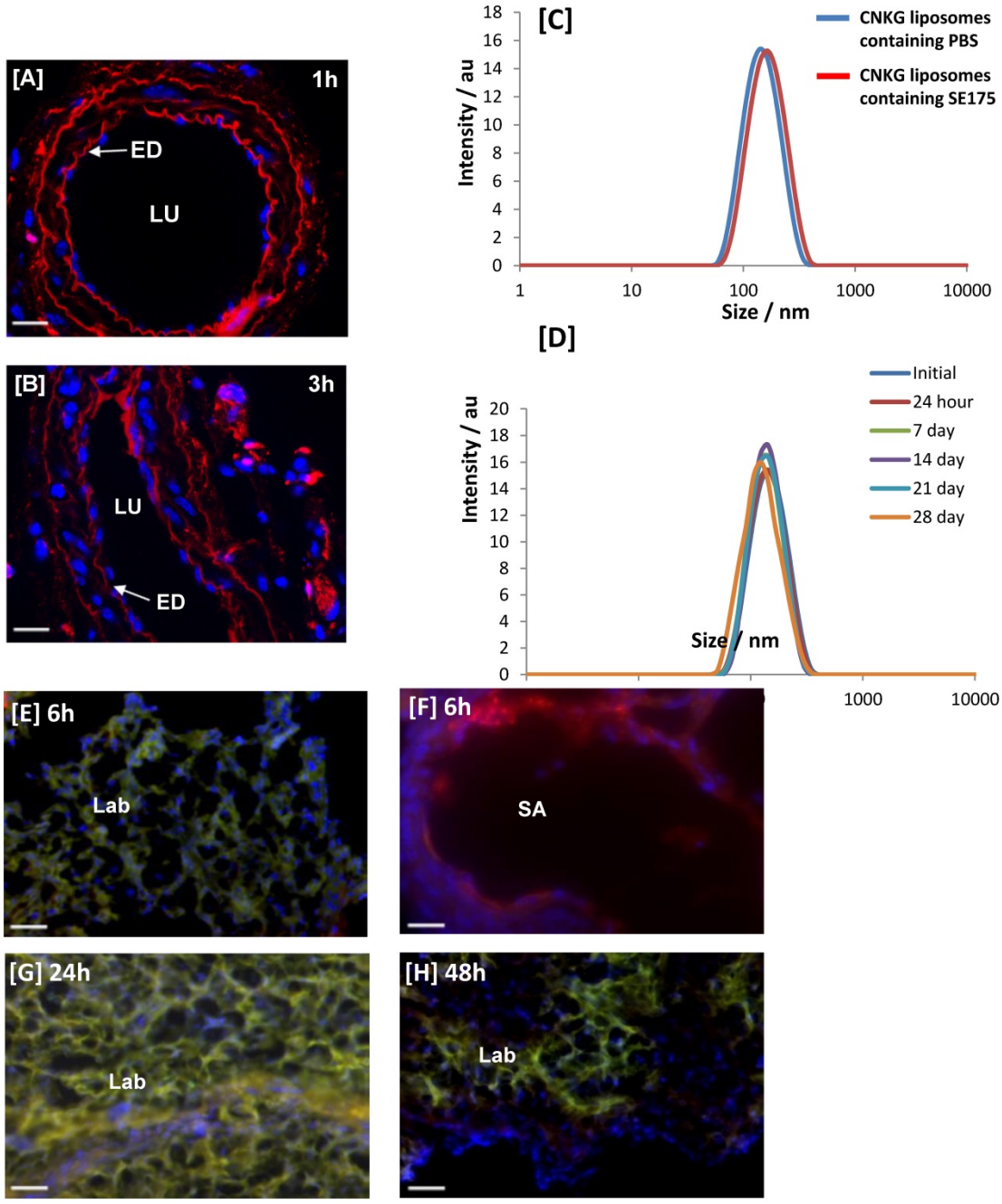


**Figure 2. CNKGLRNK binding to uteroplacental tissue *in vitro* and *in vivo* [A, B]** Segments of mouse uterine artery were incubated with Rh-CNKGLRNK (0.27 µmol/L; red) for up to 3 h. Peptide binding and uptake was assessed by fluorescence microscopy (n = 3). Representative images are shown. Rh-labelled peptides, red; DAPI (nuclei), blue. ED = endothelium; LU = lumen. Scale bar = 50 µm. **[C]** Size distribution of freshly prepared Rh-CNKGLRNK-decorated liposomes containing either PBS (blue) or SE175 (red). A representative plot from n = 3 liposome preparations is shown. **[D]** Size distribution of Rh-CNKGLRNK–decorated liposomes containing PBS over a 28 day period (n=3). Representative plots from one preparation are shown. **[E – H]** Placentas from pregnant C57BL/6J mice collected at E18.5, following tail vein injection of Rh-CNKGLRNK (red)-decorated liposomes composed of NBD-labelled lipids (green), 6h, 24h or 48h prior to tissue harvest. Cardiac perfusion was performed to remove unbound peptide; organs were removed and assessed by fluorescence microscopy. Yellow, co-localisation of peptide (red) and lipid (green) fluorescence. Blue, DAPI (nuclei). SA, spiral artery; LB, labyrinth. Scale bars = 50 µm. n = 3 placentas from n = 3 mice per treatment group were examined. Representative images are shown.

To validate liposome targeting *in vivo*, Rh-CNKG-coupled liposomes prepared using fluorescent NBD lipids (green) were injected intravenously into pregnant mice at E15.5 and allowed to circulate for 6 h, 24 h or 48 h. Colocalisation of peptide and lipid fluorescence was observed in the placental labyrinth and the decidual spiral arteries (Figure 2E-H), with a pattern of localisation similar to free NKG peptide. Fluorescence was not observed in the maternal heart, lungs, brain or in any fetal tissues; however a transient signal was seen in the maternal liver, kidney and spleen (Supplementary Figure 1), in line with previous reports of non-specific uptake of nanoparticles by the clearance organs [42].

### The nitroxyacylated thiosalicylate SE175 induces dilation of uteroplacental arteries in mice and humans

Free SE175 was applied in increasing concentrations to freshly isolated uterine arteries from C57BL/6J and eNOS$^{-/-}$ mice, or human chorionic plate arteries from healthy term placentas, pre-constricted with phenylephrine. SE175 induced a significant, dose-dependent relaxation of C57BL/6J and chorionic plate vessels (Figure 3A, B), compared to untreated arteries and arteries treated with vehicle control; at a concentration of $10^{-5}$ M, SE175 induced a significant time-dependent relaxation of eNOS$^{-/-}$ uterine arteries (Figure 3C). Similarly, when encapsulated in CNKG-decorated liposomes, $10^{-5}$ M SE175 induced a significant, time-dependent relaxation of C57BL/6J and chorionic plate arteries, compared to untreated vessels and those treated with the vehicle control (Figure 3D, E).

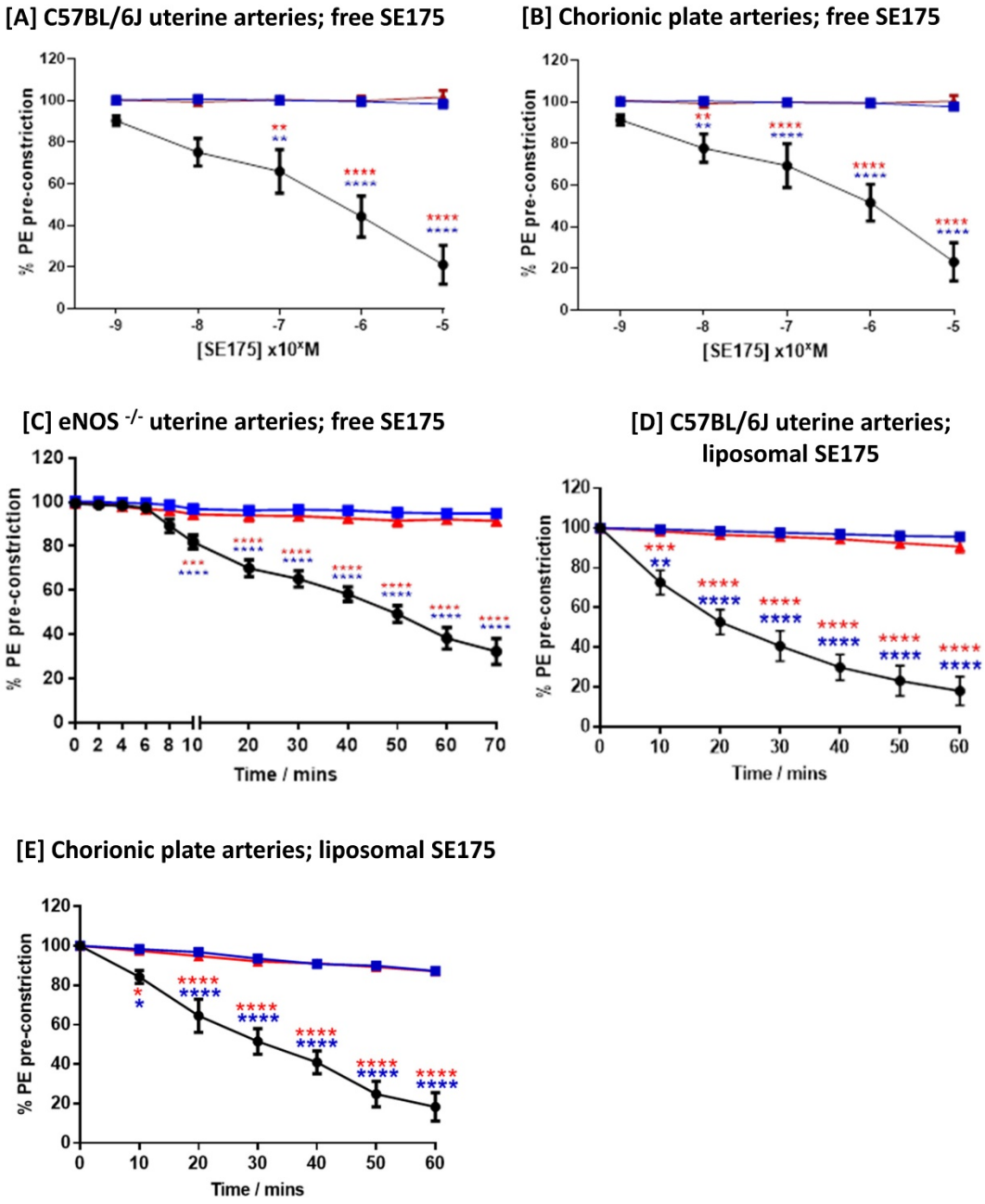


**Figure 3. Human and mouse vessels relax in response to SE175 *ex vivo* [A, D]** C57BL/6J mouse uterine arteries, **[B, E]** human term placental chorionic plate arteries, and **[C]** eNOS$^{-/-}$ mouse uterine arteries were collected, the arteries dissected and mounted onto a wire myograph. Vessels were pre-constricted with phenylephrine and vessel relaxation to **[A - C]** free or **[D, E]** liposomally-encapsulated SE175 was recorded. **[A, B]** Dose-dependent relaxation; **[C-E]** time-dependent relaxation to $10^{-5}$ M SE175. SE175 (black circles, n = 6), DMSO (blue squares, n = 6), time control (no treatment; red triangles, n = 6). Mean ± SEM; error bars not visible if smaller than symbol. Dose response curves were compared using two-way ANOVA with Bonferroni's post hoc test. **P<0.001, ***P<0.0008, ****P<0.0001.

### Targeted delivery of SE175 increases fetal weight, placental efficiency and decidual spiral artery diameter in eNOS$^{-/-}$ mice

To determine whether SE175 could increase fetal growth by enhancing uteroplacental blood flow, pregnant wild-type C57BL/6J mice were intravenously injected with PBS, PBS-loaded CNKG-decorated liposomes, SE175-loaded CNKG-decorated liposomes or free SE175 on E11.5, E13.5, E15.5 and E17.5 of pregnancy. Whilst the treatments were well tolerated and did not significantly alter litter size or proportion of resorptions, targeted delivery of SE175 to the uteroplacental vasculature did not significantly alter fetal or placental weights, and administration of free SE175 modestly but significantly decreased fetal weight (Supplementary Figure 2). In contrast, when administered to eNOS$^{-/-}$ mice, a model of pre-pregnancy hypertension and FGR, targeted SE175 increased fetal weight (Figure 4A); no other treatment had a significant effect. Fetuses from eNOS$^{-/-}$ mice had a mean weight 13 % lower than that of C57BL/6J mice; targeted delivery of SE175 increased mean fetal weight by 4 % compared to PBS-treated eNOS$^{-/-}$ mice. After targeted SE175 treatment no fetuses fell below the 5$^{th}$ or 10$^{th}$ weight centiles, thresholds that are commonly used clinically to define FGR (Figure 4B). Importantly, fewer fetuses with the lowest weights were observed in the treatment group, whereas the number of fetuses of appropriate weight was not changed (Figure 4A). In addition, no treatment significantly altered litter size or the resorption rate (Supplementary Figure 3). This suggests that targeted delivery of SE175 increases the weight of the smallest fetuses, without causing detrimental overgrowth of the heavier fetuses.

eNOS$^{-/-}$ placentas were on average 6 % heavier than those of healthy C57BL/6J; targeted delivery of SE175 significantly reduced placental weight by an average of 9 %, compared to PBS-treated eNOS$^{-/-}$ mice (Figure 4C). Placental efficiency, described in terms of the fetal:placental weight ratio, was on average 18 % lower in PBS-treated eNOS$^{-/-}$ mice than in PBS-treated C57BL/6J mice; targeted delivery of SE175 significantly increased F:P weight ratio in eNOS$^{-/-}$ mice by an average of 15 % compared to PBS treatment (Figure 4D). Delivery of free SE175 also significantly decreased placental weight and enhanced fetal:placental weight ratio compared to controls, but this improvement in placental efficiency did not translate into increased fetal weights.

Maternal blood is supplied to the placenta via the decidual spiral arteries. Quantification of mean arterial diameter revealed that eNOS$^{-/-}$ arteries were on average 28 % narrower than those of C57BL/6J; targeted delivery of SE175 significantly increased spiral artery diameter by an average of 33 % compared to PBS-treated eNOS$^{-/-}$ mice, and 17 % compared to PBS liposome-treated eNOS$^{-/-}$ mice (Figure 4E). Systemically administered SE175 had no significant effect on mean arterial diameter. All of the observed effects were independent of fetal sex.

### Targeted delivery of SE175 significantly reduces placental oxidative stress

Placentas from treated eNOS$^{-/-}$ mice were immunostained for the lipid peroxidation product 4-hydroxynonenal (4-HNE), as a marker of oxidative stress; PBS-treated C57BL/6J mice were also included for comparison. HNE immunoreactivity was observed throughout the decidua, junctional zone and labyrinth of vehicle treated eNOS$^{-/-}$ mouse placentas. The area of immunopositive tissue was quantified and expressed as a ratio of the total tissue area; targeted delivery of SE175 significantly reduced the area of placental 4-HNE immunostaining, suggestive of a reduction in lipid peroxidation in eNOS$^{-/-}$ mice (Figure 5A). No significant differences were observed in any other treatment groups. Placentas were also immunostained for COX-1 and COX-2; immunoreactivity was observed throughout the decidua, junctional zone and labyrinth of eNOS$^{-/-}$ placentas. Targeted delivery of SE175 also significantly reduced the area of COX-1 and COX-2 immunostaining (Figure 5B, C), and no treatment significantly increased COX expression, lending support to the safety of treatment. The observed effects were independent of fetal sex.

### SE175 does not alter human placental growth or function *ex vivo*

To determine whether targeted delivery of SE175 would detrimentally affect human trophoblast function, Rh-CNKG and SE175 were incubated with human placental explants. Rh-CNKG exhibited cell-penetrating properties, binding to and accumulating within the outer syncytiotrophoblast (STB) layer of first trimester explants within 30 minutes (Figure 6A), and to a lesser extent in the STB of term placental explants (Figure 6B); minimal penetration of the peptide into the underlying villous stroma was observed in either tissue. These results suggested that SE175 would be delivered to the placental surface if administered via CNKG-loaded liposomes. To determine whether SE175 treatment altered any important parameters of placental growth or function, term explants were treated with SE175 for 24 h; the nitric oxide donor SNAP was included as a positive control. SE175 treatment did not significantly

alter the rate of amino acid transport, as measured by $Na^+$-dependent $^{14}C$ meAIB uptake (Figure 6C), hCG secretion, a measure of trophoblast cell differentiation (Figure 6D), the basal rate of proliferation (Figure 6E) or apoptosis (Figure 6F).

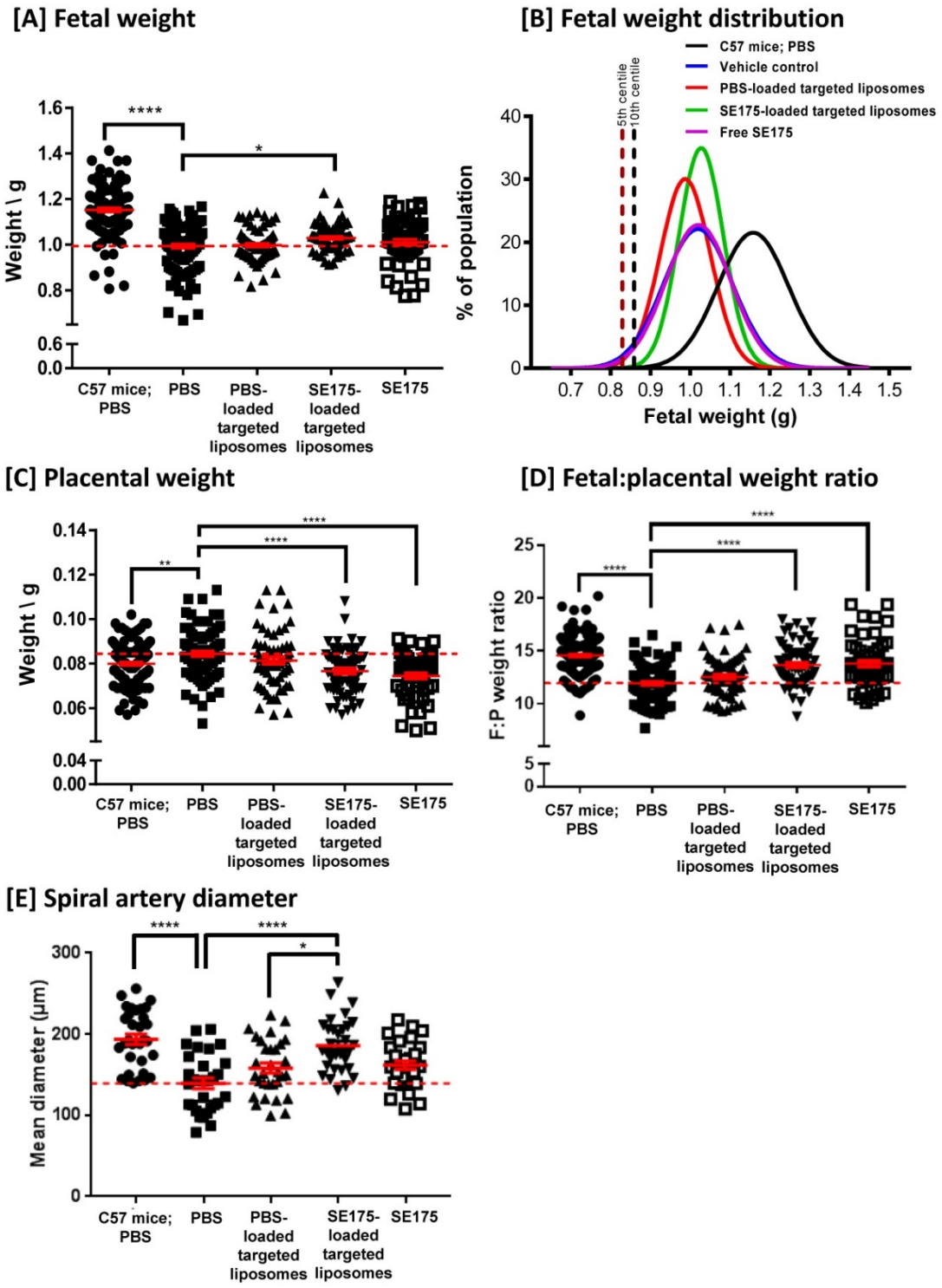


**Figure 4: Targeted delivery of SE175 increases fetal weight and placental efficiency in eNOS$^{-/-}$ mice.** eNOS$^{-/-}$ (N = dams, n = fetuses) were intravenously injected with 100 µL of PBS (N = 14, n = 113; closed black square), CNKGLRNK-decorated liposomes containing PBS (N = 9, n = 67; upward facing black triangle), CNKGLRNK-decorated liposomes containing SE175 (N = 10, n = 68; downward facing black triangle) or free SE175 (N = 8, n = 57; open black square). Data from PBS-treated C57BL/6J mice are shown for comparison (N = 17, n = 115; closed black circle). **[A]** Fetal weights, **[B]** curve fits to fetal weight distributions, **[C]** placental weights, **[D]** fetal:placental weight ratio (F:P), **[E]** spiral artery diameter (n = 3 placentas from N = 3 mice were assessed). Data points represent individual fetuses, placentas or arteries; mean ± SEM. Horizontal red dashed line represents vehicle control mean. Means were compared using one-way ANOVA with Dunnett's post hoc test. *P<0.05, **P<0.006, ****P<0.0001.

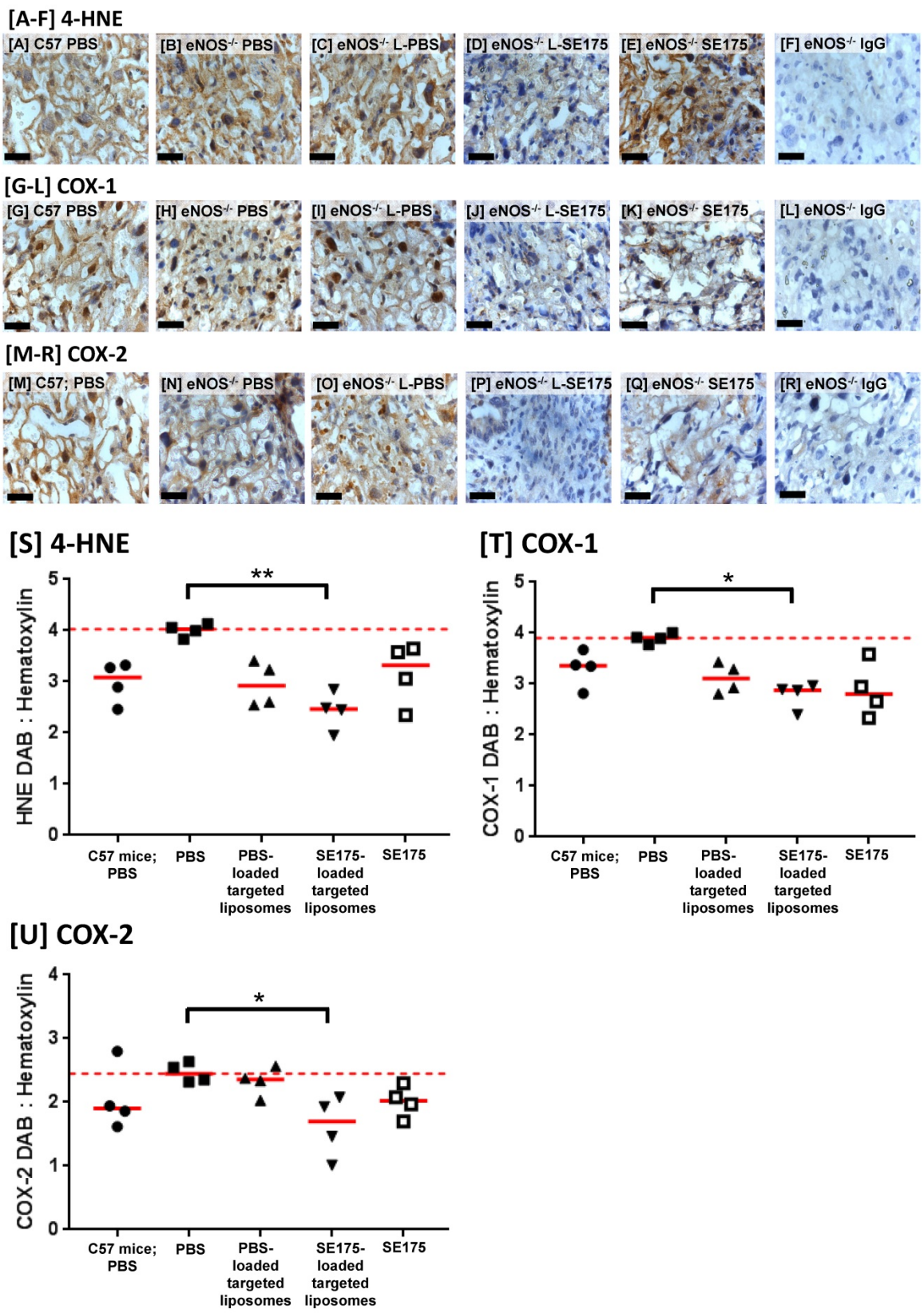


**Figure 5. Targeted delivery of SE175 reduces expression of the oxidative stress markers 4-HNE, COX-1 and COX-2 in eNOS$^{-/-}$ mice** Immunostaining of the mouse placental labyrinth with antibodies to **[A – F]** 4-HNE; **[G – L]** COX-1; **[M – R]** COX-2. **[A, G, M]** PBS-treated C57BL/6J mice, **[B, H, N]** PBS-treated eNOS$^{-/-}$ mice; **[C, I, O]** eNOS$^{-/-}$ mice treated with CNKGLRNK-decorated liposomes containing PBS (L-PBS); **[D, J, P]** eNOS$^{-/-}$ mice treated with CNKGLRNK-decorated liposomes containing SE175 (L-SE175); **[E, K, Q]** eNOS$^{-/-}$ mice treated with free SE175; **[F, L, R]** eNOS$^{-/-}$ mice, IgG control. Blue = hematoxylin; Brown = DAB; scale bars = 50 µm. n = 3 placentas from N = 4 mice were assessed; representative images are shown. **[S-U]** Quantitative assessment of DAB:Hematoxylin ratio of total area of **[S]** HNE; **[T]** COX-1; **[U]** COX-2. Mean ± SEM. Horizontal red dashed line represents vehicle control mean. Means were compared using a Kruskal Wallis test with Dunnett's post hoc test. *P<0.05; **P<0.01.

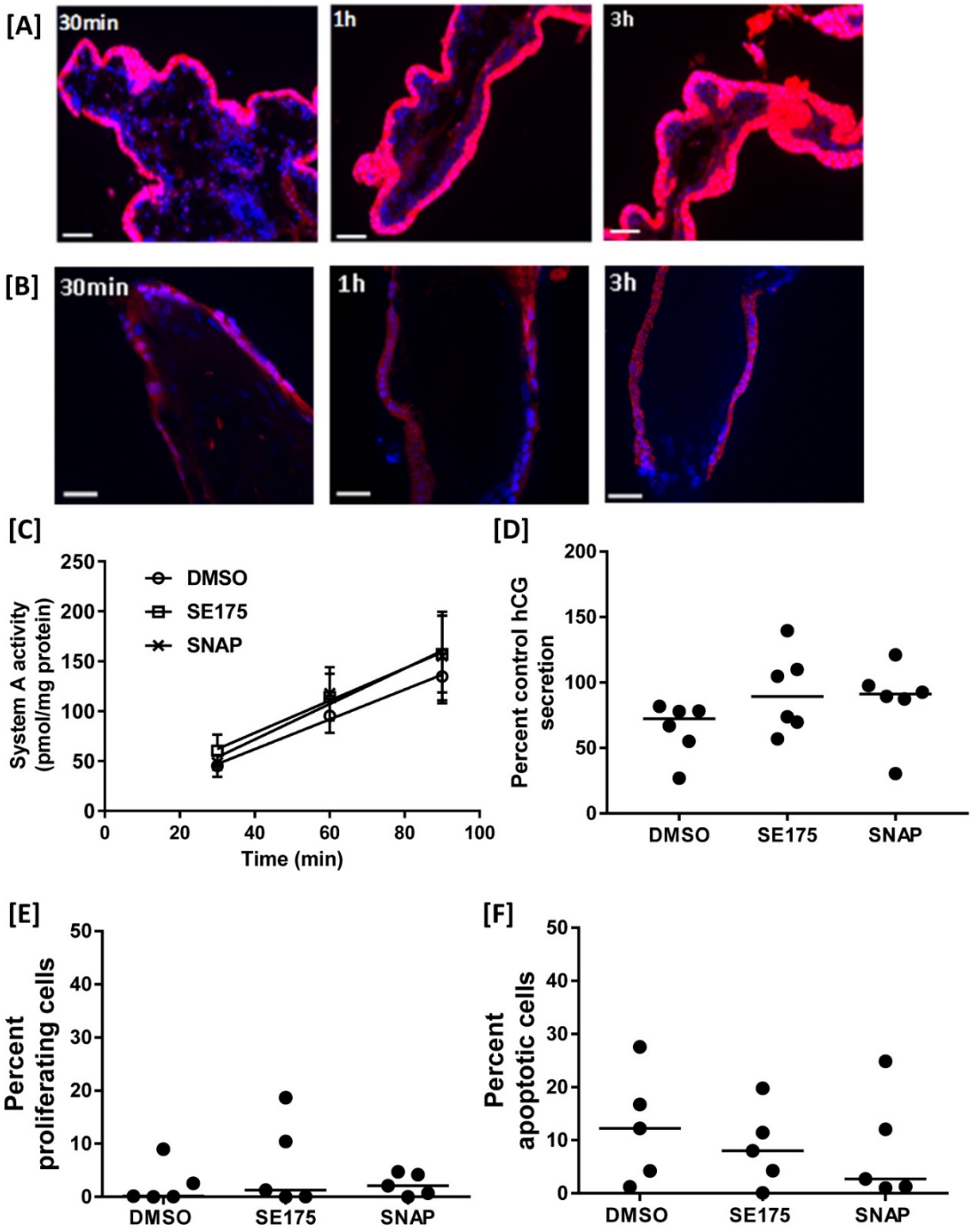


**Figure 6: SE175 does not alter human placental growth or function [A]** First trimester and **[B]** term human placental explants were incubated with Rh-CNKGLRNK (0.27 μmol/L) for up to 3 h. Peptide binding and uptake were assessed by fluorescence microscopy; (n = 3). Representative images are shown. Rh-labelled peptides, red; DAPI (nuclei), blue. ST = syncytium; VS = villous stroma; scale bar = 50 μm. **[C-F]** Term placental explants were treated with DMSO (vehicle control), SE175 or the nitric oxide donor SNAP for 24h. **[C]** $Na^+$-dependent [$^{14}$C]MeAIB uptake at 30, 60 and 90 min; mean ±SEM; n = 6. **[D]** Percent control hCG secretion as measured by ELISA; mean, n = 6. **[E]** Percent of Ki67-positive (in-cycle) cells; mean, n = 5. **[F]** Percent of M30-positive (apoptotic) cells; mean, n = 5.

## Discussion

Here we present evidence that the placental-specific homing peptide sequence CNKGLRNK acts as an efficient cell-penetrating peptide and can be conjugated to biocompatible liposomes. The resultant preparation selectively binds to the outer syncytiotrophoblast layer of human placenta *ex vivo,* and to the maternal uterine arteries and vasculature of the placental labyrinth in mice. We show that a novel vasodilator compound, the NO donor SE175, is able to induce vasodilation of mouse uterine arteries and human chorionic plate arteries *ex vivo*. We detected no adverse effect of SE175 on

several parameters of human placental growth and function and peptide-decorated liposomes encapsulating SE175 are well tolerated by pregnant mice. Finally, targeted delivery of SE175 to pregnant eNOS$^{-/-}$ mice, which exhibit dysregulated vascular function and FGR, enhances fetal growth such that the smallest fetuses are elevated above the tenth centile of weight, a commonly used clinical definition of growth restriction. Placental weight is decreased and placental efficiency is significantly enhanced. Furthermore, mean spiral artery diameter is significantly increased, and placental expression of the oxidative stress markers COX-1, COX-2 and HNE is significantly reduced, suggestive of enhanced uteroplacental perfusion.

FGR is a significant cause of stillbirth, neonatal morbidity and mortality [1,2], as well as developmental programming, which increases the risk of chronic diseases in adulthood [43]. As management strategies are limited and there are currently no therapeutics licensed for use, it is of utmost importance to identify new approaches for the treatment of FGR *in utero*. A major barrier to drug development in obstetrics is the risk of side effects in mother or fetus. A strategy that has proven useful in limiting off-target side effects of chemotherapy has been the development of targeted drug delivery systems [10]. We have previously demonstrated the potential of peptide-conjugated liposomes as a means of selectively delivering a drug payload to the placenta, resulting in enhanced fetal growth in the absence of systemic side effects. We showed that targeted placental delivery of insulin-like growth factor-II (IGF-II) was more effective than systemically administered free IGF-II in improving fetal growth in the P0 mouse model of FGR [16]. That work used a previously identified tumour-homing sequence that exhibited high affinity for uteroplacental tissues. In the present study, we took a different approach, using phage screening to identify novel homing sequences that selectively target the maternofetal interface in mice. Multiple rounds of phage biopanning led to the identification of numerous sequences with specificity for the uteroplacental vasculature; of the individual sequences tested, NKGLRNK exhibited the high degree of specificity for this vascular bed, and was not observed in fetal tissues, so was selected for incorporation into our liposome formulation. Interestingly, when using these nanoparticles for SE175 delivery, we observed comparable results to King *et al.* (2016): targeted SE175 significantly increased mean fetal weight and appeared to be of most benefit to the smallest fetuses within each litter, yet the weight of the largest fetuses was not increased. This suggests that like targeted IGF-II [16], targeted SE175 acted preferentially on fetuses at most need of a growth stimulus, namely those in which growth restriction equated to a widely accepted clinical definition of FGR. We hypothesize that maternal and/or placental regulatory mechanisms exist to prevent overgrowth of healthy fetuses in response to external stimuli; thus, the beneficial effects of SE175 were limited to the smallest placentas and fetuses within the litter.

There is accumulating evidence in humans that impaired blood flow through the uteroplacental unit occurs in some cases of FGR [4], and that abnormal vascular anatomy [17,44] and impaired myometrial and chorionic plate vascular function contribute to the underlying pathophysiology [18-22]. In parallel, there has been increasing interest in the use of vasodilators such as sildenafil citrate [26-28], carbon monoxide [45-47] and hydrogen sulphide [48-50] as putative therapeutics in mice and humans. However, these compounds are not without side effects; maternal sildenafil citrate administration impaired fetal aortic vascular function, reduced fetal glucose tolerance and caused elevated blood pressure in adulthood in mice [27,31], and caused fetal cerebral blood overflow in the pregnant rabbits [51]. In mice, carbon monoxide exposure in pregnancy has been linked to increased resorptions [52], fetal skeletal variants [53], gross fetal malformations [52] and learning impairment in offspring [54]. Hydrogen sulphide is a mucous membrane and respiratory tract irritant and an inhibitor of the cytochrome c oxidase system that can cause anoxia. Thus, we sought to examine the therapeutic potential of another compound, the nitric oxide donor SE175 [55]. SE175 has a short half-life *in vivo* and therefore a short diffusion distance once released. As it spontaneously liberates NO following cleavage by cell-surface esterases, development of tolerance is much less likely than with traditional nitrate-based therapies [56]. Here we demonstrate that both free- and liposomally encapsulated SE175 causes vasorelaxation of pre-constricted mouse wild-type and eNOS$^{-/-}$ uterine arteries and human chorionic plate arteries. Furthermore, SE175 did not detrimentally alter the basal rate of proliferation, apoptosis, differentiation or amino acid transport in human term placental explants, nor alter placental growth and function in mice, suggesting it may be a promising candidate for use in women. As NO has been implicated as a regulator of a number of important trophoblast functions including cell turnover, invasion and protection from apoptosis [57-59], this is a very positive outcome.

*In vivo*, targeted delivery of SE175 significantly decreased placental expression of the oxidative stress marker 4-HNE, an unsaturated hydroxyalkenal that is

produced by lipid peroxidation in cells. Oxidative stress has previously been shown to induce upregulation of COX enzyme expression in the mouse placenta [37]; in our study, expression of COX-1 and COX-2 was also reduced by SE175. These findings imply that either SE175 significantly enhanced local blood flow to reduce oxidative stress, or that it exhibits additional antioxidant properties. Given that liposomally-encapsulated SE175 also increased mean spiral artery diameter, this provides more evidence for improved uteroplacental perfusion following administration of SE175. Suboptimal placental function is characterised by increased placental oxidative stress [60] which in turn can lead to vascular dysfunction [61], so this observation highlights another potential benefit of SE175.

It has been hypothesised that the salicylate-like breakdown product of SE175 may act as an inhibitor of cyclooxygenase (COX) activity [55]. As COX-1 expression is elevated in the placentas of women with pre-eclampsia [62], and COX inhibition improves fetal growth and attenuates late gestational hypertension in mice [63], we sought to examine whether SE175 exerts beneficial effects on human placental growth and function that are additional to those associated with the NO donor SNAP, which does not inhibit COX. There was no significant difference between the effects of SNAP and SE175 on trophoblast turnover, amino acid uptake or hCG secretion in human term placental explants; thus, either SE175 did not reach a concentration high enough to inhibit COX activity, or COX inhibition had no effect on the parameters tested.

Much of the previous work on targeted nanoparticles has focussed on delivery of chemotherapeutics to tumours; as such, the biocompatibility and safety of the nanocarriers has been considered of lesser importance, with any reduction in systemic side effects being regarded as advantageous. Moreover, as the primary aim is to eliminate the tumour cells, any tissue-specific cytotoxicity is viewed as an additional positive outcome. The evaluation of nanoparticle effects on the placenta and its vasculature requires a more rigorous approach to the detection of toxicity. Studies of nanoparticle biodistribution and fetoplacental toxicity in pregnancy have determined the effects of size, surface charge and composition on outcome (reviewed by [64]). The emerging picture indicates that the majority of the nanoparticles assessed, including quantum dots, silica, gold and iron oxide nanoparticles, exhibit significant placental transfer, fetal accumulation and cytotoxicity. Thus, liposomes represent an attractive option for nanoparticle-mediated placental drug targeting. The peptide-decorated liposomes used in this study did not cross the placenta, did not accumulate in fetal tissues and repeated administration did not cause any apparent fetal toxicity or physical deformities. In addition, treated dams did not display any signs of distress, and gross morphological analysis of maternal organs indicated no apparent abnormalities. Litter size and the number of resorptions were similar between treatment groups. However, since sequential measurements cannot be taken from the same animal with the methodologies used in this study, additional work is required to further understand nanoparticle absorption, distribution, metabolism and excretion, along with a detailed study of neonatal outcome.

Development of novel therapeutics for use in pregnancy is an area that has historically proved difficult to translate from the bench to the clinic. However, there is now a precedent for this: sildenfil citrate [65] and melatonin [66] are undergoing clinical trials for treatment of fetal growth restriction [67], and a novel vascular endothelial growth factor (VEGF) adenoviral gene therapy, which significantly increases uterine blood flow and fetal growth in guinea pigs and sheep, is being tested in humans [68-71]. Thus, our novel system for selectively targeting the uteroplacental vasculature and identification of SE175 as a safe and effective uteroplacental vasodilator holds much promise for the future.

## Abbreviations

4-HNE: 4-hydroxynonenal; CNKG: CNKGLRNK; COX-1: cyclooxygenase-1; COX-2: cyclooxygenase-2; DAB: diaminobenzidine; DPSC: 1,2-distearoyl-*sn*-glycero-3-phosphocholine; DSPE-PEG: 1,2-distearoyl-*sn*-glycero-3-phosphoethanolamine-N-[amino(polyethylene glycol)]; E: embryonic day; eNOS$^{-/-}$: endothelial nitric oxide synthase knockout; FAM: 5(6)–carboxyfluorescein; FGR: fetal growth restriction; IGF-II: insulin-like growth factor-II; JZ: junctional zone; Lab: labyrinth; NKG:NKGLRNK; NO: nitric oxide; rh: rhodamine; SA: spiral artery; SE175: 2-[[4-[(nitrooxy)methyl]benzoyl]thio]-benzoic acid methyl ester; SNAP: S-nitroso-N-acetylpenicillamine; STB: syncytiotrophoblast; VEGF: vascular endothelial growth factor.

## Supplementary Material

Supplementary figures.
http://www.thno.org/v07p3715s1.pdf

## Acknowledgements

The authors thank the research midwives of St. Mary's Hospital for their assistance in obtaining placentas and the staff at the Biological Services Facility, University of Manchester.

## Sources of funding

This research was funded by a BBSRC David Phillips Fellowship to LKH (BB/H022627/1), a BBSRC DTP studentship to NC and a R01 CA 152327 from the US National Cancer Institute to ER. The Maternal and Fetal Health Research Centre is supported by funding from Tommy's the Baby Charity, an Action Research Endowment Fund, the Manchester Biomedical Research Centre and the Greater Manchester Comprehensive Local Research Network.

## Competing Interests

The authors have declared that no competing interest exists.

## References

1. MacKay AP, Berg CJ, Atrash HK. Pregnancy-related mortality from preeclampsia and eclampsia. Obstetrics and gynecology. 2001; 97: 533-8.
2. Bernstein IM, Horbar JD, Badger GJ, Ohlsson A, Golan A. Morbidity and mortality among very-low-birth-weight neonates with intrauterine growth restriction. The Vermont Oxford Network. Am J Obstet Gynecol. 2000; 182: 198-206.
3. Gluckman PD, Hanson MA, Cooper C, Thornburg KL. Effect of in utero and early-life conditions on adult health and disease. The New England journal of medicine. 2008; 359: 61-73.
4. Alberry M, Soothill P. Management of fetal growth restriction. Archives of disease in childhood Fetal and neonatal edition. 2007; 92: F62-7.
5. Garite TJ, Clark R, Thorp JA. Intrauterine growth restriction increases morbidity and mortality among premature neonates. Am J Obstet Gynecol. 2004; 191: 481-7.
6. Fisk NM, Atun R. Systematic analysis of research underfunding in maternal and perinatal health. BJOG : an international journal of obstetrics and gynaecology. 2009; 116: 347-56.
7. Fisk NM, Atun R. Market failure and the poverty of new drugs in maternal health. PLoS Med. 2008; 5: e22.
8. Pasqualini R, Ruoslahti E. Organ targeting in vivo using phage display peptide libraries. Nature. 1996; 380: 364-6.
9. Rajotte D, Arap W, Hagedorn M, Koivunen E, Pasqualini R, Ruoslahti E. Molecular heterogeneity of the vascular endothelium revealed by in vivo phage display. J Clin Invest. 1998; 102: 430-7.
10. Ruoslahti E, Bhatia SN, Sailor MJ. Targeting of drugs and nanoparticles to tumors. J Cell Biol. 2010; 188: 759-68.
11. Accardo A, Morelli G. aReview peptide-targeted liposomes for selective drug delivery: advantages and problematic issues. Biopolymers. 2015; 104: 462-79.
12. Gray BP, Li S, Brown KC. From phage display to nanoparticle delivery: functionalizing liposomes with multivalent peptides improves targeting to a cancer biomarker. Bioconjug Chem. 2013; 24: 85-96.
13. She ZG, Hamzah J, Kotamraju VR, Pang HB, Jansen S, Ruoslahti E. Plaque-penetrating peptide inhibits development of hypoxic atherosclerotic plaque. J Control Release. 2016; 238: 212-20.
14. Hamzah J, Kotamraju VR, Seo JW, Agemy L, Fogal V, Mahakian LM, et al. Specific penetration and accumulation of a homing peptide within atherosclerotic plaques of apolipoprotein E-deficient mice. Proc Natl Acad Sci U S A. 2011; 108: 7154-9.
15. Ferretti C, Bruni L, Dangles-Marie V, Pecking AP, Bellet D. Molecular circuits shared by placental and cancer cells, and their implications in the proliferative, invasive and migratory capacities of trophoblasts. Hum Reprod Update. 2007; 13: 121-41.
16. King A, Ndifon C, Lui S, Widdows K, Kotamraju VR, Agemy L, et al. Tumor-homing peptides as tools for targeted delivery of payloads to the placenta. Science advances. 2016; 2: e1600349.
17. Junaid TO, Brownbill P, Chalmers N, Johnstone ED, Aplin JD. Fetoplacental vascular alterations associated with fetal growth restriction. Placenta. 2014; 35: 808-15.
18. Sweeney M, Wareing M, Mills TA, Baker PN, Taggart MJ. Characterisation of tone oscillations in placental and myometrial arteries from normal pregnancies and those complicated by pre-eclampsia and growth restriction. Placenta. 2008; 29: 356-65.
19. Wareing M, Greenwood SL, Fyfe GK, Baker PN. Reactivity of human placental chorionic plate vessels from pregnancies complicated by intrauterine growth restriction (IUGR). Biol Reprod. 2006; 75: 518-23.
20. Mills TA, Wareing M, Bugg GJ, Greenwood SL, Baker PN. Chorionic plate artery function and Doppler indices in normal pregnancy and intrauterine growth restriction. Eur J Clin Invest. 2005; 35: 758-64.
21. Corcoran J, Lacey H, Baker PN, Wareing M. Altered potassium channel expression in the human placental vasculature of pregnancies complicated by fetal growth restriction. Hypertens Pregnancy. 2008; 27: 75-86.
22. Jones S, Bischof H, Lang I, Desoye G, Greenwood SL, Johnstone ED, et al. Dysregulated flow-mediated vasodilatation in the human placenta in fetal growth restriction. J Physiol. 2015; 593: 3077-92.
23. Jones CJ. Mechanisms of transfer across the human placenta. In: Polin A, Fox, editor. Fetal and Neonatal Physiology. Elsevier; 2011: 133-45.
24. Swanson AM, David AL. Animal models of fetal growth restriction: Considerations for translational medicine. Placenta. 2015; 36: 623-30.
25. Krishna U, Bhalerao S. Placental insufficiency and fetal growth restriction. Journal of obstetrics and gynaecology of India. 2011; 61: 505-11.
26. Dastjerdi MV, Hosseini S, Bayani L. Sildenafil citrate and uteroplacental perfusion in fetal growth restriction. Journal of research in medical sciences : the official journal of Isfahan University of Medical Sciences. 2012; 17: 632-6.
27. Dilworth MR, Andersson I, Renshall LJ, Cowley E, Baker P, Greenwood S, et al. Sildenafil citrate increases fetal weight in a mouse model of fetal growth restriction with a normal vascular phenotype. PloS one. 2013; 8: e77748.
28. Stanley JL, Andersson IJ, Poudel R, Rueda-Clausen CF, Sibley CP, Davidge ST, et al. Sildenafil citrate rescues fetal growth in the catechol-O-methyl transferase knockout mouse model. Hypertension. 2012; 59: 1021-8.
29. Stanley JL, Sulek K, Andersson IJ, Davidge ST, Kenny LC, Sibley CP, et al. Sildenafil Therapy Normalizes the Aberrant Metabolomic Profile in the Comt(-/-) Mouse Model of Preeclampsia/Fetal Growth Restriction. Scientific reports. 2015; 5: 18241.
30. Renshall L, Dilworth M, Cottrell E, Garrod A, Cowley E, Greenwood S, et al. Female offspring from sildenafil citrate-treated pregnancies exhibit impaired glucose tolerance. Placenta. 2014; 35: A41-A.
31. Renshall LJ, Dilworth MR, Greenwood SL, Sibley CP, Wareing M. In vitro assessment of mouse fetal abdominal aortic vascular function. American journal of physiology Regulatory, integrative and comparative physiology. 2014; 307: R746-54.
32. Kulandavelu S, Qu D, Adamson SL. Cardiovascular function in mice during normal pregnancy and in the absence of endothelial NO synthase. Hypertension. 2006; 47: 1175-82.
33. van der Heijden OW, Essers YP, Fazzi G, Peeters LL, De Mey JG, van Eys GJ. Uterine artery remodeling and reproductive performance are impaired in endothelial nitric oxide synthase-deficient mice. Biology of reproduction. 2005; 72: 1161-8.
34. Poudel R, Stanley JL, Rueda-Clausen CF, Andersson IJ, Sibley CP, Davidge ST, et al. Effects of resveratrol in pregnancy using murine models with reduced blood supply to the uterus. PLoS One. 2013; 8: e64401.
35. Hefler LA, Reyes CA, O'Brien WE, Gregg AR. Perinatal development of endothelial nitric oxide synthase-deficient mice. Biology of reproduction. 2001; 64: 666-73.
36. Kusinski LC, Stanley JL, Dilworth MR, Hirt CJ, Andersson IJ, Renshall LJ, et al. eNOS knockout mouse as a model of fetal growth restriction with an impaired uterine artery function and placental transport phenotype. American journal of physiology Regulatory, integrative and comparative physiology. 2012; 303: R86-93.
37. Burdon C, Mann C, Cindrova-Davies T, Ferguson-Smith AC, Burton GJ. Oxidative stress and the induction of cyclooxygenase enzymes and apoptosis in the murine placenta. Placenta. 2007; 28: 724-33.
38. Teesalu T, Sugahara KN, Kotamraju VR, Ruoslahti E. C-end rule peptides mediate neuropilin-1-dependent cell, vascular, and tissue penetration. Proc Natl Acad Sci U S A. 2009; 106: 16157-62.
39. Teesalu T, Sugahara KN, Ruoslahti E. Mapping of vascular ZIP codes by phage display. Methods in enzymology. 2012; 503: 35-56.
40. Wareing M, Crocker IP, Warren AY, Taggart MJ, Baker PN. Characterization of small arteries isolated from the human placental chorionic plate. Placenta. 2002; 23: 400-9.
41. Kusinski LC, Baker PN, Sibley CP, Wareing M. In vitro assessment of mouse uterine and fetoplacental vascular function. Reproductive sciences. 2009; 16: 740-8.
42. Takahashi D, Azuma H, Sakai H, Sou K, Wakita D, Abe H, et al. Phagocytosis of liposome particles by rat splenic immature monocytes makes them transiently and highly immunosuppressive in ex vivo culture conditions. The Journal of pharmacology and experimental therapeutics. 2011; 337: 42-9.
43. Galjaard S, Devlieger R, Van Assche FA. Fetal growth and developmental programming. J Perinat Med. 2013; 41: 101-5.
44. Chen CP, Bajoria R, Aplin JD. Decreased vascularization and cell proliferation in placentas of intrauterine growth-restricted fetuses with abnormal umbilical artery flow velocity waveforms. American journal of obstetrics and gynecology. 2002; 187: 764-9.
45. Linzke N, Schumacher A, Woidacki K, Croy BA, Zenclussen AC. Carbon monoxide promotes proliferation of uterine natural killer cells and remodeling of spiral arteries in pregnant hypertensive heme oxygenase-1 mutant mice. Hypertension. 2014; 63: 580-8.
46. Venditti CC, Casselman R, Murphy MS, Adamson SL, Sled JG, Smith GN. Chronic carbon monoxide inhalation during pregnancy augments uterine artery blood flow and uteroplacental vascular growth in mice. American journal of physiology Regulatory, integrative and comparative physiology. 2013; 305: R939-48.

47. Venditti CC, Casselman R, Young I, Karumanchi SA, Smith GN. Carbon monoxide prevents hypertension and proteinuria in an adenovirus sFlt-1 preeclampsia-like mouse model. PLoS One. 2014; 9: e106502.
48. Wang K, Ahmad S, Cai M, Rennie J, Fujisawa T, Crispi F, et al. Dysregulation of hydrogen sulfide producing enzyme cystathionine gamma-lyase contributes to maternal hypertension and placental abnormalities in preeclampsia. Circulation. 2013; 127: 2514-22.
49. Bhatia M. Hydrogen sulfide as a vasodilator. IUBMB life. 2005; 57: 603-6.
50. Thorup C, Jones CL, Gross SS, Moore LC, Goligorsky MS. Carbon monoxide induces vasodilation and nitric oxide release but suppresses endothelial NOS. The American journal of physiology. 1999; 277: F882-9.
51. Lopez-Tello J, Arias-Alvarez M, Jimenez-Martinez MA, Barbero-Fernandez A, Garcia-Garcia RM, Rodriguez M, et al. The effects of sildenafil citrate on feto?placental development and haemodynamics in a rabbit model of intrauterine growth restriction. Reproduction, fertility, and development. 2016.
52. Singh J, Aggison L, Jr., Moore-Cheatum L. Teratogenicity and developmental toxicity of carbon monoxide in protein-deficient mice. Teratology. 1993; 48: 149-59.
53. Schwetz BA, Smith FA, Leong BK, Staples RE. Teratogenic potential of inhaled carbon monoxide in mice and rabbits. Teratology. 1979; 19: 385-92.
54. Abbatiello ER, Mohrmann K. Effects on the offspring of chronic low exposure carbon monoxide during mice pregnancy. Clinical toxicology. 1979; 14: 401-6.
55. Endres S, Hacker A, Noack E, Kojda G, Lehmann J. NO-Donors, part 3: nitrooxyacylated thiosalicylates and salicylates - synthesis and biological activities(#). European journal of medicinal chemistry. 1999; 34: 895-901.
56. Munzel T, Daiber A, Mulsch A. Explaining the phenomenon of nitrate tolerance. Circulation research. 2005; 97: 618-28.
57. Dash PR, Cartwright JE, Baker PN, Johnstone AP, Whitley GS. Nitric oxide protects human extravillous trophoblast cells from apoptosis by a cyclic GMP-dependent mechanism and independently of caspase 3 nitrosylation. Experimental cell research. 2003; 287: 314-24.
58. Dash PR, Cartwright JE, Whitley GS. Nitric oxide inhibits polyamine-induced apoptosis in the human extravillous trophoblast cell line SGHPL-4. Human reproduction. 2003; 18: 959-68.
59. Belkacemi L, Bainbridge SA, Dickinson MA, Smith GN, Graham CH. Glyceryl trinitrate inhibits hypoxia/reoxygenation-induced apoptosis in the syncytiotrophoblast of the human placenta: therapeutic implications for preeclampsia. Am J Pathol. 2007; 170: 909-20.
60. Myatt L, Cui X. Oxidative stress in the placenta. Histochemistry and cell biology. 2004; 122: 369-82.
61. Myatt L, Kossenjans W, Sahay R, Eis A, Brockman D. Oxidative stress causes vascular dysfunction in the placenta. The Journal of maternal-fetal medicine. 2000; 9: 79-82.
62. Wetzka B, Nusing R, Charnock-Jones DS, Schafer W, Zahradnik HP, Smith SK. Cyclooxygenase-1 and -2 in human placenta and placental bed after normal and pre-eclamptic pregnancies. Human reproduction. 1997; 12: 2313-20.
63. Sones JL, Cha J, Woods AK, Bartos A, Heyward CY, Lob HE, et al. Decidual Cox2 inhibition improves fetal and maternal outcomes in a preeclampsia-like mouse model. JCI insight. 2016; 1.
64. Muoth C, Aengenheister L, Kucki M, Wick P, Buerki-Thurnherr T. Nanoparticle transport across the placental barrier: pushing the field forward! Nanomedicine. 2016; 11: 941-57.
65. Ganzevoort W, Alfirevic Z, von Dadelszen P, Kenny L, Papageorghiou A, van Wassenaer-Leemhuis A, et al. STRIDER: Sildenafil Therapy In Dismal prognosis Early-onset intrauterine growth Restriction--a protocol for a systematic review with individual participant data and aggregate data meta-analysis and trial sequential analysis. Systematic reviews. 2014; 3: 23.
66. Alers NO, Jenkin G, Miller SL, Wallace EM. Antenatal melatonin as an antioxidant in human pregnancies complicated by fetal growth restriction - a phase I pilot clinical trial: study protocol. BMJ open. 2013; 3: e004141.
67. Cottrell EC, Sibley CP. From pre-clinical studies to clinical trials: generation of novel therapies for pregnancy complications. Int J Mol Sci. 2015; 16: 12907-24.
68. Sheppard M, Spencer RN, Ashcroft R, David AL, Consortium E. Ethics and social acceptability of a proposed clinical trial using maternal gene therapy to treat severe early-onset fetal growth restriction. Ultrasound Obstet Gynecol. 2016; 47: 484-91.
69. Mehta V, Abi-Nader KN, Peebles DM, Benjamin E, Wigley V, Torondel B, et al. Long-term increase in uterine blood flow is achieved by local overexpression of VEGF-A(165) in the uterine arteries of pregnant sheep. Gene Ther. 2012; 19: 925-35.
70. Carr DJ, Mehta V, Wallace JM, David AL. VEGF gene transfer to the utero-placental circulation of pregnant sheep to enhance fetal growth. Methods Mol Biol. 2015; 1332: 197-204.
71. Mehta V, Carr DJ, Swanson A, David AL. VEGF gene transfer to the utero-placental circulation of pregnant guinea pigs to enhance fetal growth. Methods Mol Biol. 2015; 1332: 189-96.
72. Lundberg JO, Weitzberg E, Gladwin MT. The nitrate-nitrite-nitric oxide pathway in physiology and therapeutics. Nature reviews. Drug discovery, 2008;7(2): 156-167.